Intermetallic Clathrates Revisited

Michael Baitinger, Umut Aydemir, Bodo Böhme, Horst Borrmann, Ulrich Burkhardt, Wilder Carrillo-Cabrera, Arnold Guloy[1], Frank Haarmann, Walter Jung[2], Kirill Kovnir[3], Lien Nguyen Thi Kim, Reiner Ramlau, Walter Schnelle, Ulrich Schwarz, Andrei Shevelkov[4], Zhongjia Tang[1], Igor Veremchuk, Julia Zaikina[3], and Yuri Grin

Numerous investigations of new intermetallic clathrates have been undertaken during the past years. Most of these research activities have been promoted in particular by the growing demand for thermoelectric materials [1]. However, it was more and more realized that the reported physical properties measured on bulk samples can differ substantially from the intrinsic properties of homogeneous samples with specific composition. Especially the role of vacancies in the clathrate frameworks is commonly overlooked in the interpretation of X-ray diffraction results. Depending on the vacancy concentration, however, compounds of similar composition can show either *n*-type or *p*-type conduction, even metallic or semiconducting properties. Crystallographically, they can form different superstructures with characteristic defect ordering. A reliable knowledge of these properties is decisive for the applicability of a thermoelectric material as much as for the understanding of complex structure-property relations. In order to meet the required standard of investigations, the thorough characterization of clathrates developed into a joint field of cross-disciplinary research at our institute. During the last two years our main emphasis was the development of new preparation routes for intermetallic compounds in general, and for intermetallic clathrates in particular.

The first boron containing clathrate

The four-bonded host framework of the clathrate-I structure can entirely be formed with the valence electrons of group 14 elements. In the binary silicon clathrates $M_{8-x}Si_{46}$, the additional valence electrons of the guest metal atoms occupy antibonding states and the compounds show metallic behavior. Semiconducting clathrates have often been obtained by partial substitution of group 14 atoms in the host framework by trivalent group 13 atoms, e.g., in $Rb_8Ga_8Si_{38}$ [2] or in $Eu_8Ga_{16}Ge_{30}$ [3]. However, the substitution by boron in a clathrate structure was achieved only recently for the first time [4]. $K_7B_7Si_{39}$ is the first borosilicide with a clathrate-type crystal structure (Fig. 1) featuring the smallest lattice parameter ever observed for clathrate-I compounds based on group 14 elements (a = 9.952(1) Å, space group $Pm\bar{3}n$). This result came as a surprise because borosilicides typically form different kinds of structure types containing interconnected B_{12} icosahedral clusters. The distinct contraction of the framework in boron containing clathrates is of special interest for the preparation of clathrate compounds with smaller metal cations (such as rare earth elements) which have been only rarely obtained up to now.

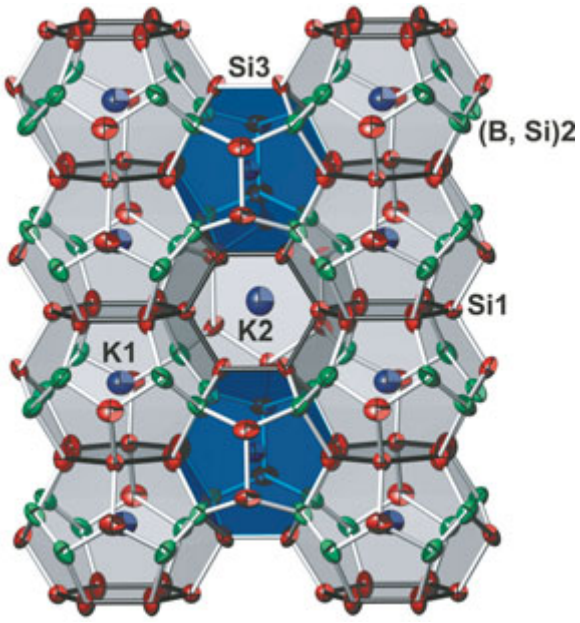

Fig. 1: Crystal structure of $K_7B_7Si_{39}$ along [100]. Green: (Si + B) at site 16i, red: Si at 24k and 6c sites, blue: K at 2a und 6d sites. Dodecahedra are drawn in blue, tetrakaidekahedra in grey.

According to the observed lattice parameters, $K_7B_7Si_{39}$ represents the boron-rich border of a narrow homogeneity range towards a higher Si : B ratio. $K_7B_7Si_{39}$ forms well-shaped crystals (Fig. 2). This is unusual since silicon clathrates are normally obtained as fine, polycrystalline powders by

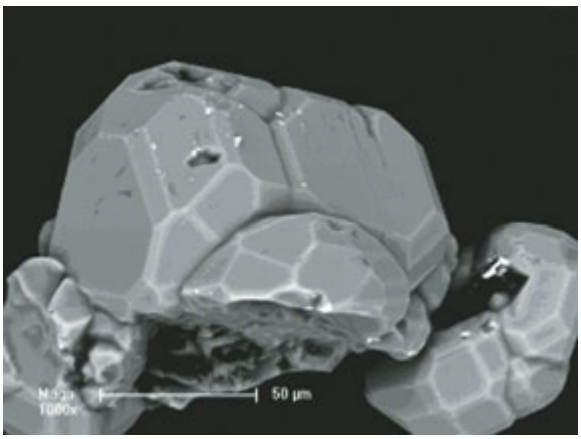

Fig. 2: SEM image of $K_7B_7Si_{39}$ crystals.

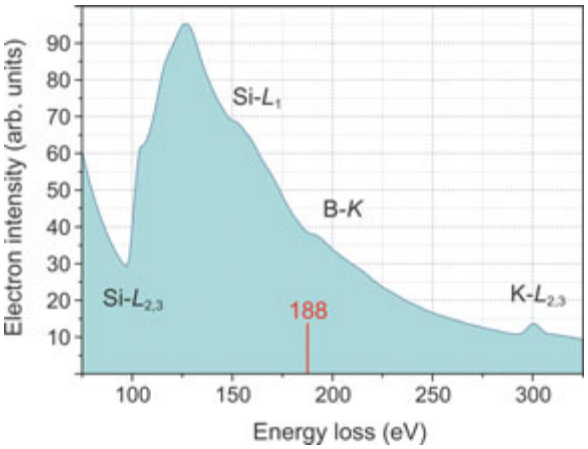

Fig. 3: EEL spectrum of $K_7B_7Si_{39}$. Crystallite in [111] orientation, boron K edge at 188 eV.

thermal decomposition or oxidation of reactive educts. The presence of boron in the clathrate phase was qualitatively established by EDXS investigations, while silicon and potassium were quantified close to the expected ratio. Microcrystallites representing the clathrate phase were additionally analysed by EELS. The experimental spectrum (Fig. 3) agrees well with that simulated for the composition $K_7B_7Si_{39}$.

The composition $K_7B_7Si_{39}$ was established by structure determination of single-crystal X-ray diffraction data (21526 measured, 1845 independent reflections). The structure refinement reveals a full occupation of the potassium position at the crystallographic site 6*d* whereas the position 2*a* is half-filled with one K atom. The framework sites 6*c* and 24*k* are fully occupied by Si atoms, while the silicon atoms on site 16*i* are partially substituted by 6.8(3) boron atoms. In total, this results in the composition $K_{7.04(2)}B_{6.8(3)}Si_{39.2(3)}$, or, in idealized form, $K_7B_7Si_{39}$. The pure phase is diamagnetic with a weak temperature dependence of the magnetic susceptibility (χ(300 K) ≈ $-250\cdot10^{-6}$ emu/mol). The electrical resistivity is relatively large at room temperature (ρ(300) = 3 mΩ m) and increases with decreasing temperature. These observations are characteristic for a heavily doped semiconductor. The observed electronic transport properties agree with the long relaxation time found in NMR experiments. The equilibrium magnetization in ^{11}B-NMR experiments is achieved after 60 s which is clearly longer than the typical relaxation time for a material with metallic conductivity. This supports the results of the crystal structure determination which gave equal numbers of boron and potassium atoms. This allows $K_7B_7Si_{39}$ to be interpreted as a Zintl phase.

Clathrates containing transition metal elements

In contrast to the silicon based compounds, clathrates of the heavier group 14 elements Ge and Sn may contain voids, □, in the framework of covalently bonded atoms. In this case, the valence electrons of the guest metal atoms are formally transferred to threefold bonded anions (3b)Ge^- or (3b)Sn^-, surrounding the voids. In the compound $K_8Ge_{44}\square_2$, for example, two defects and eight (3b)Ge anions per unit cell are formed corresponding to the valence electrons of 8 K atoms [5]. Thus, the charge balance can be written as $[K^+]_8[(3b)Ge^-]_8[(4b)Ge^0]_{36}$. In the clathrate-I phases of the system Ba-Ni-Ge, substitution atoms and defects occur together in the same compound. Therefore, the determination of the chemical composition is considerably aggravated. This system was chosen as a model compound within the European Network of Excellence CMA to reinvestigate in detail the relation between physical properties, chemical composition and crystal structure. The homogeneity range was determined to be $Ba_8Ni_xGe_{41.8+\Delta y}$ ($0.6 < x \leq 4.2$; $|\Delta y| < 1$) and its structure characterized (space group $Pm\bar{3}n$, a = 10.657(1) - 10.681(1) Å). The homogeneity range was confirmed by EDX and EELS. The chemical composition can be derived from an idealized Zintl-Phase of composition $Ba_8Ge_{42}\square_4$ in which the structure defects □ can successively be filled by Ni atoms. Samples with composition $Ba_8Ni_{3.5}Ge_{42}$ (a = 10.681(1) Å) were prepared from the melt at 1113(5) K. For lower Ni contents ($0 < x \leq 0.6$) a 2 × 2 × 2 super cells (space group

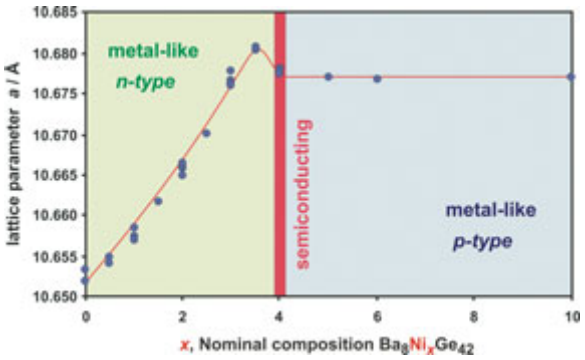

Fig. 4: Lattice parameters and electrical conductivity within the homogeneity range $Ba_8Ni_{4.2-x}Ge_{41.8+\Delta y}$.

$Ia\bar{3}d$, a = 21.307(2) Å) were obtained indicating a solid solution of Ni into the binary $Ba_8Ge_{43}\square_3$.

DC resistivity measurements of samples with composition $Ba_8Ni_{4.0}Ge_{42}$ exhibit semiconducting behavior, while samples with other compositions can be classified as "bad metals" ($d\rho/dT > 0$). Samples with lower Ni content than $Ba_8Ni_{4.0}Ge_{42}$ show *n*-type, samples with higher Ni content *p*-type conduction (Fig. 4).

New type - I clathrates with group 9 and 10 elements were synthesized, namely $Ba_8CoGe_{43-x}\square_{2+x}$ ($Pm\bar{3}n$, a = 10.670(1) Å), $Ba_8RhGe_{43-x}\square_{2+x}$ ($Pm\bar{3}n$, a = 10.688(1) - 10.698(1) Å), $Ba_8Rh_2Si_{44}$ ($Pm\bar{3}n$, a = 10.347(1) Å) and $Ba_8Ni_xSi_{46-x}$ ($2.4 \leq x \leq 3.7$; $Pm\bar{3}n$, a = 10.290(1) Å - 10.301(1) Å). The huge variety of compositions which can be achieved in transition-metal substituted clathrates will be used to tune the charge carrier concentration and hence, the thermoelectric activity. These experiments are important to improve the applicability of clathrates as thermoelectric materials.

A clathrate III compound with unusually high thermal stability

A necessary precondition for thermoelectric heat conversion is the thermal stability of the material at operating temperature. In fact, the application range covered by commercial thermoelectric materials is already restricted to temperatures below 300 °C. The new clathrate III, $Si_{130}P_{42}Te_{21}$, was synthesized from the elements ($P4_2/mnm$ a = 19.2632(3) Å, c = 10.0706(2) Å) as a single phase and exhibits the highest thermal stability ever reported for this class of materials (~ 1240 °C under vacuum, 1230 °C in air) [6]. This opens new perspectives for the preparation of clathrate-based

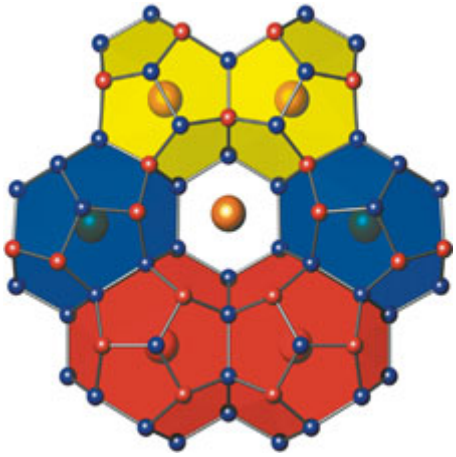

Fig. 5: Polyhedral packing in the clathrate III structure of $Si_{130}P_{42}Te_{21}$ with condensed 20-, 24- and 26-vertex cages.

materials for high-temperature applications. Single crystal X-ray diffraction and solid state ^{31}P-NMR revealed a non-random distribution of phosphorus atoms over the framework positions. The composition of this novel clathrate is in accordance with the Zintl rule, and was confirmed by wavelength dispersive X-ray spectroscopy (WDXS) as well as the semiconducting transport behavior.
So far, $Cs_{30}Na_{(1.33x-10)}Sn_{(172-x)}$ [7] and $Si_{130}P_{42}Te_{21}$ are the only examples for intermetallic clathrate III compounds the crystal structures of which are derived from the bromine hydrate $[(Br_2)_{20}\square_{10}](H_2O)_{172}$ (Fig. 5).

Metastable clathrates obtained by oxidation reactions

A novel low-temperature method for the preparation of clathrates, the oxidation of reactive precursor compounds, was recently developed at our institute. The new element modification Ge(*cF*136) with a clathrate-II-type crystal structure was synthesized by the protic oxidation of $Na_{12}Ge_{17}$ at 300 °C in an ionic liquid of DTAC/$AlCl_3$ [8]. The acidic protons are delivered by the β-H-acidic agent DTAC which undergoes a Hofmann elimination under the conditions of the reaction. By means of a similar preparation method, the new binary $K_{8.6(4)}Ge_{136}$ ($Fd\bar{3}m$, a = 15.302(1) Å) has been synthesized [9]. The precursor K_4Ge_9 was oxidized in the ionic liquid DTAC/$AlCl_3$ at 300 °C to an X-ray amorphous product. Crystalline samples of $K_{8.6(4)}Ge_{136}$ were obtained after subsequent annealing of the crude

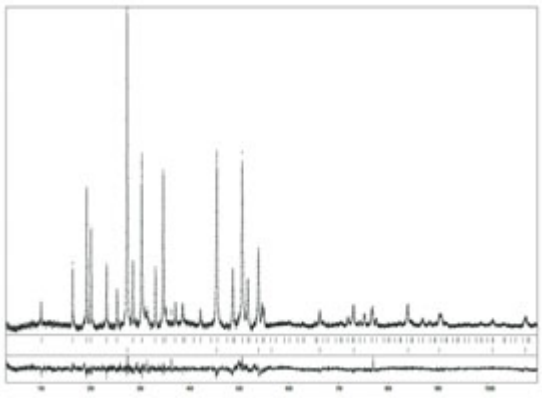

Fig. 6: X-ray powder diffraction pattern of $K_{8.6(4)}Ge_{136}$: experimental data (top) and the difference curve (bottom). Crystalline α-Ge was found as a minor phase (~4 mass-%).

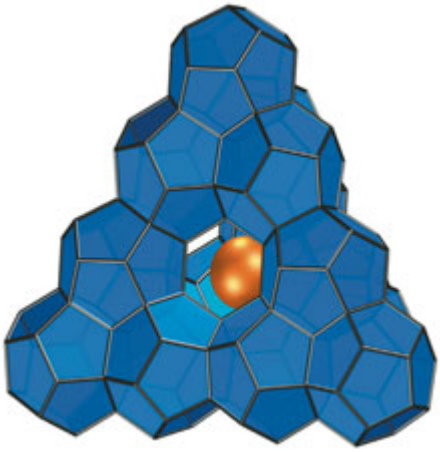

Fig. 7: Crystal structure of the type-II clathrate $K_{8.6(4)}Ge_{136}$. Ge_{20} polyhedra are shown blue, E_{24} polyhedra (open) are filled by K atoms (golden).

product in Ar at 370 °C (Fig. 6). The composition was determined from X-ray powder diffraction and confirmed by EDXS analysis either on clathrate crystallites in a transmission electron microscope, or on bulk material in a scanning electron microscope. In the clathrate II structure of $K_{8.6(4)}Ge_{136}$, the K atoms preferably occupy the larger Ge_{28} cages rather than the Ge_{20} cages (Fig. 7). $K_{8.6(4)}Ge_{136}$ is the first example of a clathrate-II crystal structure containing K atoms. The compound is metastable and was found to decompose exothermically at 471 °C.

The deeper understanding of the heterogeneous character of the oxidation led to a further development of the synthesis method and the controlled oxidation of precursor compounds with oxidizing gases, e.g., HCl:

$M_4Si_4 + HCl \rightarrow M_{8-x}Si_{46} + MCl + H_2$

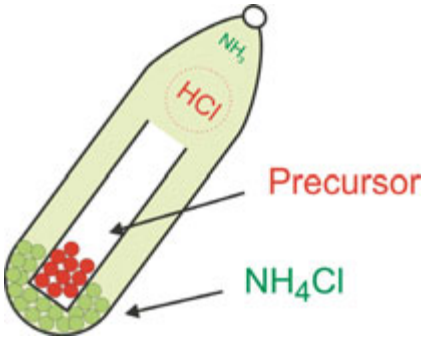

Fig. 8: Schematic experimental setup for the oxidation of precursor compounds with gaseous HCl.

The preparation route can be varied by the choice of the HCl source, e.g., gaseous HCl can be produced by dissociation of NH_4Cl. The precursor compound and NH_4Cl have to be placed in separate vessels (Fig. 8). For the first time, the type-I clathrates $Na_{6.2}Si_{46}$ ($Pm\bar{3}n$, a = 10.199(1) Å) and K_7Si_{46} ($Pm\bar{3}n$, a = 10.278(1) Å) have been obtained with a distinctly reduced occupancy of cage atom positions (Fig. 9). [10] The synthesis method could be extended to clathrates containing alkaline earth metals such as $Na_2Ba_6Si_{46}$ ($Pm\bar{3}n$, a = 10.281(1) Å) [11] and Ba_6Si_{46} ($Pm\bar{3}n$, a = 10.274(1) Å). Especially the synthesis of Ba_6Si_{46} is remarkable because Ba/Si clathrates were exclusively produced by high pressure preparation methods up to now [12].

Further optimization of the synthesis conditions in the Na / Si system led to a considerable reduction of the sodium content. The latter was determined from crystal structure refinement. (Tab. 1).

These results indicate that it might even be feasible to prepare a new silicon allotrope Si(*cP*46) with empty clathrate-I structure by the oxidation method. This method provides a general preparation route which is scalable and allows the synthesis of large amounts of crystalline powders with standard laboratory equipment. Densification techniques of the reaction products are under investigation.

Table 1: Type-I clathrate Na_xSi_{46} obtained from oxidation reactions

Refined composition	***a* / Å**
$Na_{6.2}Si_{46}$	10.199(1)
$Na_{4.5}Si_{46}$	10.200(1)
$Na_{3.9}Si_{46}$	10.193(1)
$Na_{1.7}Si_{46}$	10.175(1)

Vacancy ordering in $K_8Sn_{44}\square_2$

The type-I clathrates $M_8Sn_{44}\square_2$ (M = K, Rb, Cs) are Zintl phases stabilized by the formation of vacancies in the covalent framework [13-16]. The real structure of clathrates and especially the ordering of defects is not yet reported in the current literature. The formation of superlattices was investigated by extended single crystal analyses of $Rb_8Sn_{44}\square_2$ and $Cs_8Sn_{44}\square_2$ ($Pm\bar{3}n$; $cP54$ → $Ia\bar{3}d$; $cI432$; 2 × 2 × 2 super cell) [17-18]. The homologue compound $K_8Sn_{44}\square_2$ forms peritectically at 390 °C from $K_{8-x}Sn_{25}$ and melt. For this compound, a primitive unit cell could be verified from single crystal data at room temperature and at 100 K [19]. However, the X-ray powder pattern could never be indexed completely by assuming a cubic unit cell. Recently, a reinvestigation of $K_8Sn_{44}\square_2$ by electron microscopy using SAED revealed the existence of a large orthorhombic polymorph with the unit cell dimensions $2a \times 2a \times 4a$ (Fig. 10) which is in agreement with the low intensity reflections observed in XRPD-patterns (Fig. 11). Because the formation of super cells depends always on the annealing temperature, similar unit cells might be also found for $Rb_8Sn_{44}\square_2$ and $Cs_8Sn_{44}\square_2$.

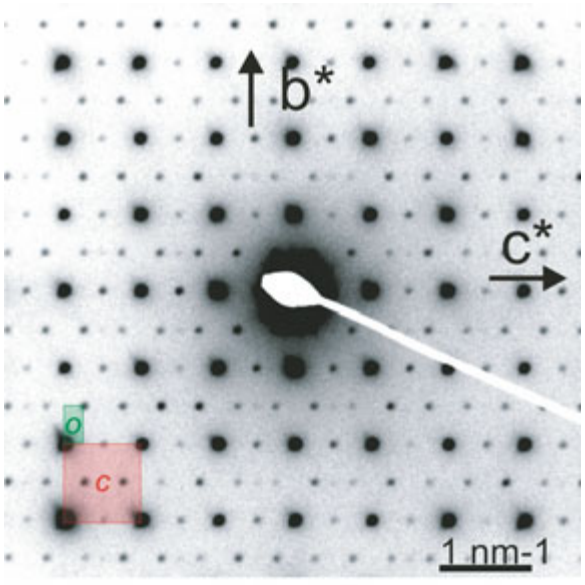

Fig. 10: SAED image of $K_8Sn_{44}\square_2$ along [100]. Vacancy ordering causes the formation of a superlattice with orthorhombic unit cell (dimensions 2a × 2a × 4a) marked in green. The cubic subcell with space group $Pm\bar{3}n$ is marked in red.

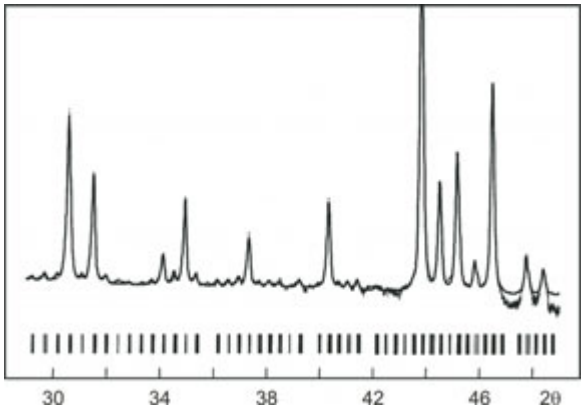

Fig. 11: X-ray powder pattern of $K_8Sn_{44}\square_2$, indexed with a orthorhombic unit cell.

Conclusion

As a result of extensive investigations in the past, intermetallic clathrates and their crystal structures were generally supposed to be well understood. However, detailed new insight reveals a subtle dependence of crystal structure, local atomic ordering, and hence, related physical properties on the precise chemical composition and preparation conditions. With the development of novel synthesis methods, clathrates with new chemical compositions can be obtained, which have not been accessible by traditional preparation methods. This opens new prospects to adjust the charge carrier concentration which is decisive for an optimization of thermoelectric properties.

References

[1] *P. Rogl* in Thermoelectrics Handbook, (ed. by D. M. Rowe), Taylor & Francis, Chap. 32, 2006
[2] *H. G. von Schnering, R. Kröner, H. Menke, K. Peters, and R. Nesper,* Z. Kristallogr. NCS **213** (1998) 677–677.
[3] *S. Paschen, W. Carrillo-Cabrera, A. Bentien, V. H. Tran, M. Baenitz, Yu. Grin, and F. Steglich,* Phys. Rev. B **64** (2001) 214404-1.
[4] *W. Jung, J. Lörincz, R. Ramlau, H. Borrmann, Yu. Prots, F. Haarmann, W. Schnelle, U. Burkhardt, M. Baitinger, and Yu. Grin,* Angew. Chem. **119** (2007) 6846-6850; Angew. Chem. Int. Ed. **46** (2007) 6725-6728.
[5] *J. Llanos,* Thesis, University of Stuttgart 1984.
[6] *J. V. Zaikina, K. A. Kovnir, F. Haarmann, W. Schnelle, U. Burkhardt, H. Borrmann, U. Schwarz, Yu. Grin, and A. V. Shevelkov,* Chem. Eur. J. **14** (2008) 5414-5422.

[7] *S. Bobev, S. C. Sevov,* J. Am. Chem. Soc. **123** (2001) 3389-3390.
[8] *A. M. Guloy, R. Ramlau, Z. Tang, W. Schnelle, M. Baitinger, Yu. Grin,* Nature **443** (2006) 320-323.
[9] *A. M. Guloy, Z. Tang, R. Ramlau, B. Böhme, M. Baitinger, and Yu. Grin,* Eur. J. Inorg. Chem., accepted.
[10] *B. Böhme, A. Guloy, Z. Tang, W. Schnelle, U. Burkhardt, M. Baitinger, and Y. Grin,* JACS, **129** (2007) 5348-5349.
[11] *B. Böhme, U. Aydemir, A. Ormeci, W. Schnelle, M. Baitinger, and Y. Grin,* Sci. Technol. Adv. Mater. **8** (2007) 410-415.
[12] *S. Yamanaka, E. Enishi, H. Fukuoka, and M. Yasukawa,* Inorg Chem. **39** (2000) 56-58.
[13] *J. T. Zhao, J. D. Corbett,* Inorg. Chem. 33 (1994) 5721-5726.
[14] *H.G. von Schnering, R. Kröner, M. Baitinger, K. Peters, R. Nesper, and Yu. Grin,* Z. Kristallogr. NCS, **215** (2000) 205-206.
[15] *C. W. Myles, J. Dong, and O. F. Sankey,* Phys. Rev. B **64** (2001) 165202.
[16] *L. Møllnitz, N. P. Blake, and H. Metiu,* J. Chem. Phys. **117** (2002) 1302-1312.
[17] *F. Dubois, T. F. Fässler,* J. Am. Chem. Soc. **127** (2005) 3264-3265.
[18] *A. Kaltzoglou, S. D. Hoffmann, and T. F. Fässler,* Eur. J. Inorg. Chem. **26** (2007) 4162 – 4167.
[19] *M. Baitinger, Yu. Grin, and H.G. von Schnering,* Book of Abstracts, VIth European Conference on Solid State Chemistry, Zürich, Sept. 17-20, 1997; PA116.

[1] Department of Chemistry and the Texas Center for Superconductivity, University of Houston, Houston, Texas 77204-5003
[2] Institut für Anorganische Chemie, Universität zu Köln Greinstrasse 6, 50939 Köln
[3] Department of Chemistry, Dittmer Bldg., Florida State University, Tallahassee, FL 32306-4390
[4] Chemistry Department, Lomonosov Moscow State University Leninskie Gory 1–3, 119991 Moscow